Reverse water gas shift in microwave plasma for O2 removal and CO2 conversion enhancement

A. Hecimovic, R. Antunes, C. Kranig, A. Meindl, Ursel Fantz

Angaben zur Veröffentlichung / Publication details:

Hecimovic, A., R. Antunes, C. Kranig, A. Meindl, and Ursel Fantz. 2026. "Reverse water gas shift in microwave plasma for O2 removal and CO2 conversion enhancement." *Journal of CO2 Utilization* 106: 103403. https://doi.org/10.1016/j.jcou.2026.103403.

Journal of CO2 Utilization 106 (2026) 103403

Contents lists available at ScienceDirect

Journal of CO2 Utilization

journal homepage: www.elsevier.com/locate/jcou

Reverse water gas shift in microwave plasma for O_2 removal and CO_2 conversion enhancement

A. Hecimovic [a,*], R. Antunes [a], C. Kranig [a], A. Meindl [a], U. Fantz [a,b]

[a] Max-Planck-Institut für Plasmaphysik, Boltzmannstraße 2, 85748 Garching, Germany
[b] AG Experimentelle Plasmaphysik, University of Augsburg, Augsburg, 86135, Germany

ARTICLE INFO

Keywords:
Reverse water gas shift
Microwave plasma
CO2 conversion
O2 removal

ABSTRACT

One of the major challenges of using plasmas for CO_2 conversion is the removal of oxygen in the plasma effluent. In this work an efficient removal of oxygen (>99% removal) from the product gas stream in a 2.45 GHz microwave plasma reactor at atmospheric pressure is reported. This is achieved by addition of H_2 gas enabling the reverse water gas shift reaction. The addition of H_2 takes place either immediately after the microwave resonator, or inside the resonator, affecting the plasma size and optical emission in the latter case. The performance is comparable for both positions of H_2 addition. Already 2 vol.% of H_2 admixture results in O_2 removal below 0.1 vol.% from the product gas stream, however at the cost of lower CO_2 conversion. An increase of H_2 flow leads to a rise of the CO_2 conversion in accordance to the thermodynamics of the reverse water gas shift reaction. CO_2 conversions of up to 65%, and CO energy yields of up to 0.27 $kg_{CO}kWh^{-1}$ are achieved with less than 0.1 vol.% O_2 in the product gas. The $[H_2]/[CO]$ ratio in the product gas lies in the range between 1.8–2.2 which makes it suitable for synthetic fuel processes such as Fischer–Tropsch. The performance comparison demonstrates that the presented method of O_2 removal by H_2 admixing to the microwave CO_2 plasma is a very efficient process compared to other O_2 removal methods yielding the highest energy yields.

1. Introduction

Plasma conversion technology is investigated as a potential technology for conversion of gases, aiming at optimising the efficiency of the process in order to replace current energy intensive technologies [1]. Microwave plasmas are one of many plasma types used for gas conversion, yielding relatively high conversion and energy efficiency values for CO_2 decomposition [2]. One of the key challenges of the plasma process, in addition to increasing the CO_2 conversion and the process efficiency, is the gas separation in the plasma effluent. In electrolytic reactors, another emerging technology for gas conversion, the products of CO_2 conversion are separated on the cathode (CO_2 and CO) and on the anode (O_2), unlike the plasma effluent which has a single outstream comprising CO, O_2 and unconverted CO_2 gases. In order to be compatible with a potential downstream process using the produced CO as a feedstock, the gas separation step is required (e.g. the Fischer–Tropsch process requires O_2 concentrations below 1 vol.% and the H_2/CO ratio in the range of 1.8–2.2 [3]). Removal of oxygen is a necessary first step since methods for separating CO and CO_2 towards pure CO already exist [4].

Several methods relying on sacrificial/reduced materials, membranes or admixing gases to remove oxygen have been investigated and are briefly discussed here. One of them involves placing a carbon bed in the plasma effluent, which enables an effective removal of oxygen upon reaction with carbon atoms. Moreover, CO_2 can react with C and form additional CO via the Boudouard reaction ($CO_2 + C \rightarrow 2CO$), thereby increasing the CO_2 conversion in a gliding arc plasma [5–7]. A demonstration of this method was reported showing an increase of the CO_2 conversion from 7.6% to 12.6 % [6] and further towards 20% [8] with efficient oxygen removal with the carbon bed placed in the effluent of the gliding arc. It is important to point out that this approach requires continuous replenishment of the carbon bed to replace the material being used in the reactions. The oxygen can also be captured using a reduced oxygen carrier (OC). Oxygen-deficient zirconium-doped ceria installed in the effluent of a rotating gliding arc (RGA) plasma has successfully demonstrated complete O_2 removal and increased CO_2 conversion up to 84 vol.% for a gas inlet composition with 5 vol.% CO_2 in Ar at 500 sccm (standard cubic centimetres per minute) [9]. Once the OC is oxidised, a reduction step has to follow to guarantee quasi-continuous operation in a plasma chemical looping

* Corresponding author.
E-mail address: Ante.Hecimovic@ipp.mpg.de (A. Hecimovic).

https://doi.org/10.1016/j.jcou.2026.103403
Received 5 January 2026; Received in revised form 9 March 2026; Accepted 19 March 2026
Available online 24 March 2026

process. An efficient method for reducing oxidised OC, closing the plasma chemical loop, and the up-scaling potential of this method has not been demonstrated yet.

Mixed ionic-electronic conductors, such as perovskite membranes exclusively permeable to O_2, have been used in the effluent of microwave plasmas, where high gas temperatures above 700 °C thermally activate the membranes for permeation of O_2 molecules [10]. Simultaneous use of 21 membranes in a plasma environment has been demonstrated to remove up to 42 sccm or 4.8% of the produced O_2 [11]. The major obstacle for this method is that a large number of membranes is required to generate an outlet gas mixture with O_2 concentration below 1 vol.%. In a similar method, an O_2-permeable perovskite electrode was used to investigate a system consisting of a microwave plasma reactor and a solid oxide electrolysis cell (SOEC). A CO_2 plasmolysis equivalent gas mixture was fed into the SOEC electrolyser resulting in O_2 removal rate up to 4 sccm [12]. This method has not yet been demonstrated in a plasma environment.

Removal of O_2 can be achieved by adding H_2-containing molecules, such as H_2 or CH_4, to the plasma process. Gas mixtures containing CO_2 and H_2 can undergo two reactions: CO_2 hydrogenation (or CO_2 methanation), where the products are CH_4 and H_2O (reaction (1)), or reverse water gas shift (RWGS), resulting in CO and H_2O (reaction (2)).

$$CO_2 + 4H_2 \rightleftarrows CH_4 + 2H_2O, \quad \Delta H^o = -164\,\mathrm{kJmol^{-1}} \tag{1}$$

$$CO_2 + H_2 \rightleftarrows CO + H_2O, \quad \Delta H^o = 41\,\mathrm{kJmol^{-1}} \tag{2}$$

Mixing of CO_2 and CH_4, a process called dry reforming of methane results in a syngas mixture of CO and H_2.

$$CO_2 + CH_4 \rightleftarrows 2CO + 2H_2, \quad \Delta H^o = 247\,\mathrm{kJmol^{-1}} \tag{3}$$

CO_2 hydrogenation is an exothermic process and favourable at low temperatures and has been widely studied with plasma–catalytic DBD reactors [13]. Use of H_2 to remove O_2 from the CO_2 plasma effluent has been discussed by Aerts et al. where modelling results predict that in a dielectric barrier discharge (DBD) at atmospheric pressure already 2 vol.% of CH_4 or 3 vol.% of H_2 can completely trap O_2 even for low CO_2 conversions of several % [14]. The trapping of O promotes the CO_2 conversion by inhibiting the recombination reaction of CO with O atoms and O_2 molecules. Reverse water gas shift has been investigated in a hybrid DBD plasma–catalyst system [15]. It had been demonstrated that by using different catalytic materials it is possible to tune the selectivity either towards CO or CH_4 production. CO_2 conversions of up to 80% and energy efficiencies up to 11% at a total flow rate of 20 sccm were reported.

RWGS is favourable at high temperatures and thus suitable to study with warm/thermal plasmas, such as gliding arcs and microwave discharges. This process has been investigated in a gliding arc at atmospheric pressure, yielding CO_2 conversions of up to 54% and energy efficiencies up to 11% at total flow rates of 200 sccm (H_2 inlet concentration of 33 vol.%) [16]. Relatively high CO_2 conversions up to 85% have been measured in a microwave torch when the H_2 is added into a CO_2 plasma to produce O_2-free streams, at a pressure of 20 mbar and flow rates up to 400 sccm [17]. In the same work, 100% selectivity towards CO at an energy efficiency of 6% was reported. In a microwave plasma torch at atmospheric pressure hydrogen has been added with aim to produce higher value chemical products [18]. It should be mentioned that RWGS is an active research line in the field of thermal catalysis [19], with the main focus on tuning the properties of catalysts towards a high CO selectivity at high CO_2 conversion [20].

The addition of CH_4 (0–30 vol.%) or C_2H_4 (0–15 vol.%) to CO_2 microwave discharges has been investigated by Kuijpers et al. in the pressure range from 150 mbar to 900 mbar [21]. The experimental results demonstrate low levels of oxygen in the effluent for small additions of hydrocarbons (1 vol.%) to CO_2 discharges. The results of a quasi-1D chemical kinetic model demonstrate that OH and H radicals dramatically decrease the CO_2 conversion and energy efficiency, and remove oxygen from the effluent completely by catalysing the recombination of CO and O_2 through the reactions $CO + OH \rightarrow CO_2 + H$ and $H + O_2 \rightarrow O + OH$. For additions of more than 5 vol.% of CH_4 or C_2H_4, the CO_2 conversion, CO yield and energy efficiencies are higher than for pure CO_2 discharges [21,22].

Recently, we have demonstrated that high CO_2 conversions at atmospheric pressure can be obtained by quickly cooling the plasma effluent and preventing CO recombination by either using a nozzle [23] or a reverse vortex with cooling channels [24]. In this work we combine the reverse vortex configuration and the H_2 addition to the 2.45 GHz microwave CO_2 plasma aimed at promoting the RWGS reaction. The goal of this work is to go beyond RWGS results reported in the literature by investigating conditions relevant for the up-scaling of the process, such as higher total flows (up to 40 slm), H_2 concentrations up to 75 vol.%, and pressures up to 900 mbar. Plasma conditions with high CO_2 conversions, negligible oxygen concentration in the effluent and a H_2/CO ratio close to 2 suitable for the Fischer–Tropsch process, are demonstrated.

2. Experimental setup

A microwave plasma torch is driven by microwaves at 2.45 GHz generated by a Muegge power supply (Type ML3000D-111TC) able to deliver up to 3 kW of power. The gas is introduced into a quartz tube with 30 mm outer and 26 mm inner diameter placed in the centre of the resonator cavity. The setup is vacuum tight and connected to a vacuum pump with a valve that enables operation in a pressure range from 50 to 950 mbar independent of the total gas flow rate. The resonator is oriented downwards in order to prevent solid or liquid products to accumulate inside the resonator. On the bottom of the resonator a reverse vortex module is mounted containing four tangentially mounted CO_2 gas inlets at an angle of 35 degrees with respect to the resonator, and a 5 mm wide nozzle in the centre acting as a gas outlet (more details of the setup can be found elsewhere [24]). The injected CO_2 gas swirls upwards along the walls of quartz tube reversing its flow direction at the resonator top, then streaming downwards though the centre of the quartz tube, eventually leaving the resonator through the nozzle of the reverse vortex module. Hydrogen gas can be introduced either in the plasma effluent, downstream of the reverse vortex module, using two radially mounted gas inlets, or through tangential gas inlets in the top part of the resonator. Both configurations are shown in Fig. 1 with pictures of the plasma inside the resonator recorded at 37.5 vol.% H_2, a pressure of 900 mbar, and a power of 1.8 kW. The difference compared to the setup used in our previous work [24] is that the reverse vortex module is used without the cooling channels. This modification is motivated by the choice to use the hot plasma effluent to promote the RWGS reaction.

The plasma emission for the experiments where H_2 is introduced in the effluent is a typical bluish glow elongated through the resonator characteristic of a pure CO_2 plasma [25]. The plasma appearance changes once H_2 is introduced in the resonator, with the plasma length shrinking to about one third of the resonator height, exhibiting a bluish glow on the lower part of the plasma and pinkish glow on top of the plasma. Fig. 2 shows optical emission spectra normalised to the band-head of the C_2 Swan band (0,0) recorded in the resonator using a low resolution overview spectrometer (Ocean Optics S2000) with line of sight acceptance area of about 5 mm in diameter collecting light from the bottom half of the resonator. The spectrum shown in Fig. 2(a) is measured in a pure CO_2 plasma, displaying C_2 Swan bands, atomic carbon and atomic oxygen lines typical of a microwave CO_2 plasma [25–27]. A very similar spectrum is shown in Fig. 2(b), obtained for the case where H_2 is introduced in the effluent. The similarity between Figs. 2(a) and (b) indicate that adding H_2 in the effluent does not affect the plasma inside the resonator. Fig. 2(c) shows the spectrum recorded during operation in CO_2 plasma with H_2 introduced in the

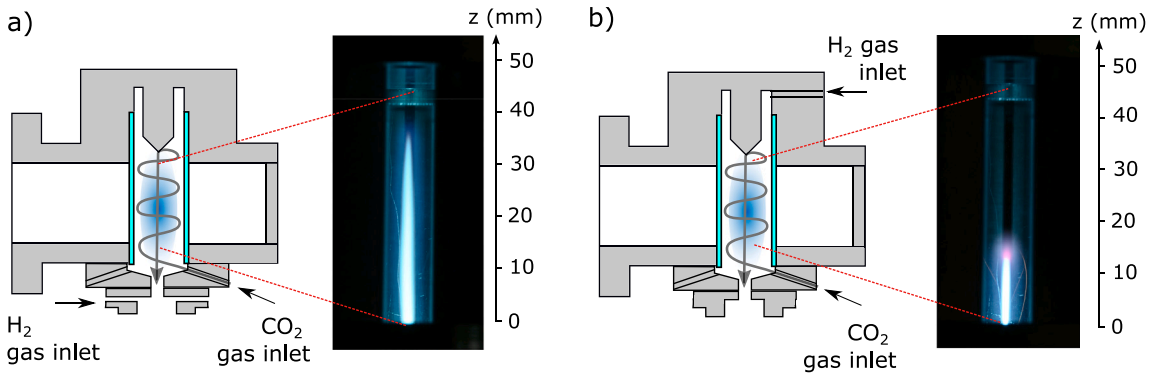

Fig. 1. Schematic of the plasma torch with CO_2 gas inlets in reverse vortex configuration with additional H_2 gas inlets placed (a) in the plasma effluent, and (b) inside the resonator. Photos of the plasma inside the resonator are shown.

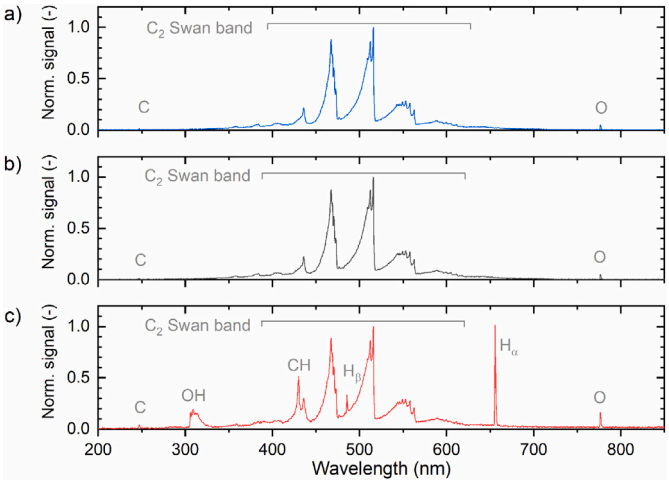

Fig. 2. Optical emission spectra recorded inside the resonator. (a) pure CO_2 plasma, (b) plasma with H_2 introduced in the plasma effluent (as in Fig. 1(a)), and (c) plasma with H_2 introduced in the resonator (as in Fig. 1(b)). The CO_2 flow rate is 10 slm, the H_2 flow rate is 6 slm, the applied power is 1.8 kW, and the pressure is 900 mbar.

resonator. In addition to the typical molecular bands and atomic lines observed in pure CO_2 plasma, additional lines belonging to OH (A-X) band, CH (A-X) band and atomic hydrogen lines are visible. This observation explains the change of the plasma emission shown in Fig. 1(b). Spatially resolved measurements of the different plasma zones inside the resonator are planned for future work.

The composition of the product gas and the CO_2 conversion are determined using a mass spectrometer (MS) downstream of the plasma where the effluent gas is well mixed and cooled close to room temperature. Notation [molecule] is used here to represent the volumetric concentration of the measured molecule in the outflow. The mass spectrometer is suitable to measure the gas composition in the pressure range 5–1000 mbar. More details of the MS can be found elsewhere [28]. Adding H_2 to the microwave plasma torch results in removal of oxygen to oxygen concentrations below 0.1 vol.%, as explained in more detail in Section 3.1. Furthermore, for all conditions investigated in this work, CH_4 concentrations are estimated to be below 0.1 vol.% and thus negligible (example is shown in Figure S4 in the supplementary material). Therefore, with CO as only carbon-containing product, the CO_2 conversion (χ_{CO_2}) is determined using the CO_{2out} and CO_{out} concentrations ([CO_{2out}] and [CO_{out}]), and considering the carbon balance.

$$\chi_{CO_2} = \frac{[CO]_{out}}{[CO_2]_{out} + [CO]_{out}} \tag{4}$$

Concentrations of water could not be correctly determined using the MS since water condenses between the plasma reactor and the measurement point, where only water vapour is detected. The following approach has been pursued to correctly account for the mass balances for C, H, O. This approach relies on using the CO_2 conversion as the quantity to estimate the outlet flow rates:

$$F^{out}_{CO_2} = F^{in}_{CO_2}(1 - \chi_{CO_2}) \tag{5}$$

$$F^{out}_{CO} = F^{in}_{CO_2} \cdot \chi_{CO_2} \tag{6}$$

$$F^{out}_{O_2} \approx 0 \tag{7}$$

$$F^{out}_{H_2O} = F^{out}_{CO} = F^{in}_{CO_2} \cdot \chi_{CO_2} \tag{8}$$

$$F^{out}_{H_2} = F^{in}_{H_2} - F^{out}_{H_2O} = F^{in}_{H_2} - F^{in}_{CO_2} \cdot \chi_{CO_2} \tag{9}$$

Eqs. (5) and (6) are those one would use for a pure CO_2 plasma. Eq. (5) determines the flow rate of CO_2 at the outlet ($F^{out}_{CO_2}$), considering some amount (χ_{CO_2}) of the inlet CO_2 got converted into CO. The CO outflow rate (F^{out}_{CO}) is in turn defined by Eq. (6) as a product of the inlet CO_2 and the CO_2 conversion. For all experiments containing H_2 the concentration of oxygen is below 0.1 vol.%, thus the O_2 outflow rate ($F^{out}_{O_2}$) is considered to be zero. Eq. (8) defines the H_2O outflow ($F^{out}_{H_2O}$) as being equal to the CO outflow rate, an approach already used in the literature [29]. This is justified as for each CO molecule produced, one oxygen atom is unaccounted for. Since no oxygen molecules have been detected, it is assumed that unaccounted oxygen atoms are bound to H_2 molecules generating water molecules. In turn, the H_2 outflow rate ($F^{out}_{H_2}$) is equal to the H_2 inlet rate reduced by the outflow rate of water.

In order to calculate the total conversion (χ_T), the H_2 conversion (χ_{H_2}) is determined using the H_2 and H_2O concentrations, considering the hydrogen balance:

$$\chi_{H_2} = \frac{[H_2O]_{out}}{[H_2]_{out} + [H_2O]_{out}} \tag{10}$$

and the total conversion (χ_T) is determined using:

$$\chi_T = [CO_2]_{in} \cdot \chi_{CO_2} + [H_2]_{in} \cdot \chi_{H_2} \tag{11}$$

with $[CO_2]_{in}$ and $[H_2]_{in}$ representing the concentrations of CO_2 and H_2 at the gas inlet, respectively. The energy efficiency with respect to the reverse water gas shift enthalpy (ΔH^0 = 41 kJmol^{-1} = 0.435 eV/molecule) is calculated as:

$$\eta_{RWGS} = \frac{\chi_T \cdot \Delta H^0}{SEI} \tag{12}$$

with SEI being the specific energy input calculated as the ratio of the power deposited in the plasma and the total input flow rate. The energy

yield is calculated as the ratio of the CO outflow rate and the power in the plasma (read from the power supply):

$$\text{Energy yield} \quad \left[\frac{\text{kg}}{\text{kWh}}\right] = 74.4 \cdot \frac{F_{CO}^{out}[\text{slm}]}{\text{Power[W]}} \tag{13}$$

Another parameter commonly used to distinguish between the chemical energy stored in the reactants and in the products is the so-called fuel efficiency [21] or fuel energy efficiency [30]. It is defined by the ratio of the useful chemical energy stored in a product to the sum of the energy stored in the reactants and the energy used to run the process.

$$\eta_f = \frac{\alpha \cdot \sum_j c_j^{out} \cdot LHV_j}{\sum_j c_j^{in} \cdot LHV_j + SEI} \tag{14}$$

with α being the correction factor to account for gas expansion [30], and c_j^{in} and c_j^{out} the in- and out-flow concentration of the molecules. LHV is the lower heating value, a measure for the energy released upon full oxidation of the specified molecule. Note that only H_2 and CO contribute for the fuel efficiency, whose values can be found in [31].

3. Results and discussion

3.1. Oxygen removal by addition of H_2

Results from the literature predict that addition of several percent of H_2 into CO_2 plasma will result in a removal of oxygen by trapping it in a water molecule, as shown in reaction (2) [14,21]. The volumetric concentrations of oxygen detected work with and without H_2 addition are presented in Fig. 3. The figure shows concentrations for different molecules measured using the mass spectrometer for H_2 inlet concentrations from 0 vol.% to 75 vol.%. For each H_2 inlet concentration a measurement interval lasting several minutes is shown. The ordinate shows the concentrations over four orders of magnitude, thus the species with concentrations lower than 0.1 vol.% show higher relative fluctuations compared to species with higher concentrations. The concentration of water in Fig. 3 is presented as equal to the concentration of CO, as described and justified in Eq. (8).

For pure CO_2 plasma large concentrations of CO_2, CO and O_2, and small quantities of H_2 are detected. The H_2 concentrations are below 0.1 vol.% and originate from the water outgassing from the surfaces inside the mass spectrometer. Adding 2 vol.% of H_2, the CO and O_2 concentrations drop significantly, while the H_2 concentration increases. Lowering of the CO concentration indicates reduced CO_2 conversion which is discussed in more detail in Section 3.3. The O_2 concentration reduces dramatically down to below 0.1 vol%, drifting below the detection limit towards the end of the measurement interval. Such low O_2 concentrations obtained with H_2 admixture demonstrate that adding H_2 to the microwave CO_2 plasma at and above 2 vol.% removes oxygen from the product gas.

3.2. Pressure variation

The CO_2 conversion in the pressure range from 200 to 950 mbar for a fixed CO_2 flow rate of 10 slm, an H_2 flow rate of 6 slm, at a constant power of 1.8 kW is shown in Fig. 4. The results consistently demonstrate that adding H_2 either in the resonator or in the effluent yield up to twice the CO_2 conversion obtained without H_2 addition. Whether the H_2 is admixed inside the resonator or added to the effluent has no effect on the CO_2 conversion. The lowest CO_2 conversion for CO_2 plasma with H_2 addition is recorded at 200 mbar. At this pressure and for H_2 injection in the resonator the plasma is more diffuse than at 900 mbar, while at pressures above 500 mbar it is contracted. For H_2 injection in the effluent, no significant change in the plasma width is observed. The photos of the plasma under these conditions can be found in the supplementary material. In presence of H_2, the CO_2 conversion increases from 200 to 500 mbar and remains constant at

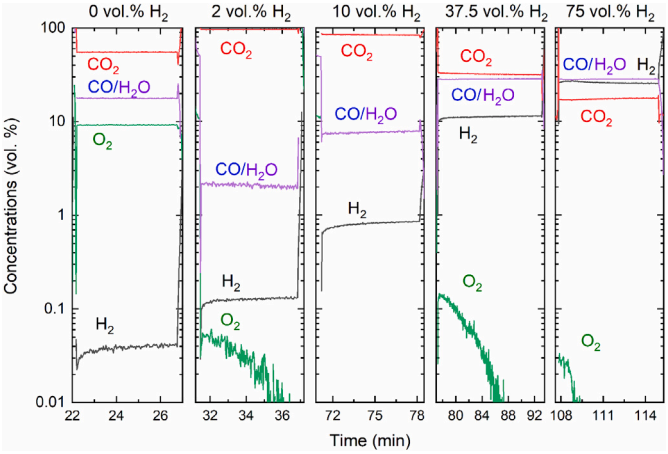

Fig. 3. The example of the concentrations for different molecules detected with the mass spectrometer for H_2 inlet concentrations between 0 vol.% and 75 vol.%.

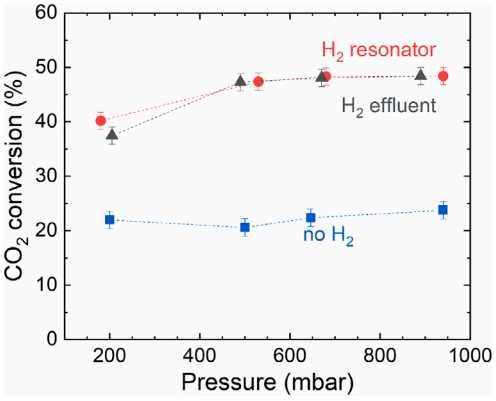

Fig. 4. CO_2 conversion at different pressures, obtained for pure CO_2 plasma (no H_2), and for CO_2 plasma with H_2 addition either in the resonator or in the effluent. The CO_2 flow rate is 10 slm, the H_2 flow rate is 6 slm, and the applied power is 1.8 kW.

higher pressures. The CO_2 conversions obtained in our previous work using the reverse vortex and cooled channels with pure CO_2 plasma yield similar results in the range 20%–25% over the pressure range 200–900 mbar for a given conditions (CO_2 flow rate of 10 slm and the applied power of 1.8 kW) [24].

3.3. H_2 concentration variation

For a fixed CO_2 flow rate, the H_2 inlet flow rate and discharge power have been varied at 500 and 900 mbar yielding results and the trends that are very similar. Due to its importance for industrial application the focus of the discussion in the following sections will be placed on the 900 mbar condition. Results obtained at 500 mbar can be found in the supplementary material. The results obtained for the H_2 flow rate variation from 0.2 slm ([H_2] of 2 vol.%) to 30 slm ([H_2] of 75 vol.%) at a fixed CO_2 flow rate of 10 slm, and a constant microwave plasma power of 1.8 kW, at 900 mbar of pressure are shown in Fig. 5. The points marked with black dots correspond to the data obtained for H_2 introduced in the effluent, and the points marked with red squares correspond to the data obtained for H_2 introduced in the resonator. The difference in CO_2 conversion obtained for the two H_2 gas inlet positions for various H_2 flow rates corroborates the finding described in the previous section that the CO_2 conversion exhibits no dependence on the H_2 delivery location. It is worth mentioning that in case of H_2

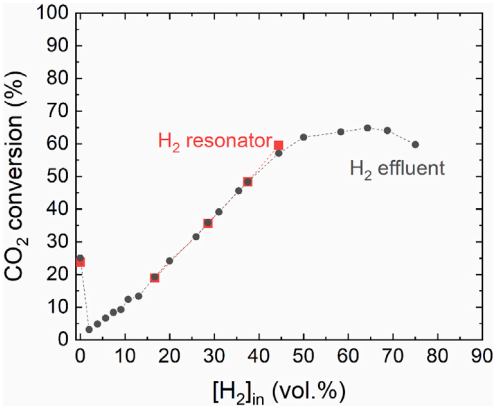

Fig. 5. CO_2 conversion as a function of H_2 inlet concentration for a fixed CO_2 flow rate of 10 slm. Black points are for the H_2 added in the effluent, and red points are for the H_2 added in the resonator. The pressure is 900 mbar, and the power is 1.8 kW.

addition inside the resonator an upper limit of about 40 vol.% H_2 inlet concentration is observed at both 500 and 900 mbar. Beyond these H_2 concentrations the plasma extinguishes.

Already a small amount of H_2 as low as 2 vol.% strongly reduces the CO_2 conversion from about 25% for a pure CO_2 plasma discharge to values in the range of several%. The behaviour of CO_2 conversion reduction for small quantities of hydrogen or hydrocarbons has already been observed in literature [17,18,21]. Increasing the H_2 concentration, the CO_2 conversion exhibits an almost linear increase for the given conditions. After $[H_2]$ = 50 vol.%, the CO_2 conversion stagnates and even reduces beyond $[H_2]$ = 70 vol.%.

In order to understand the dependence of CO_2 conversion on the H_2 concentration, thermal equilibrium calculations from 300 K to 6000 K are done with Cantera [32]. This range of temperatures is relevant since in the microwave plasma torch the gas temperatures in the centre of the plasma reach up to around 6000 K [25]. Turbulent mixing of the hot plasma gas and the colder surrounding gas in the effluent lowers the gas temperature resulting in a thermalisation of the gas at temperatures below 6000 K.

The thermal equilibrium calculations and the resulting CO_2 conversion are shown in Fig. 6. Fig. 6(a) shows an example of the molar composition of relevant species in the temperature range 300 K to 6000 K for a thermal equilibrium calculation with $[H_2]$ of 31 vol.% at 900 mbar. At temperatures up to around 500 K the methanation process dominates (reaction (1)). In the temperature range between around 1000 K and around 2200 K a quasi-plateau in the molar composition dominated by the RWGS process (reaction (2)) yielding H_2 and CO as the products is seen. Beyond about 2500 K dissociation of CO_2 and H_2O molecules into H_2, O_2, CO, OH and atoms takes place. For a given pressure, the exact ranges of the temperatures dominated by the methanation process and RWGS process depend on the CO_2 and H_2 gas mixture.

Fig. 6(b) presents the CO_2 conversion (defined by Eq. (4)) for $[H_2]$ = 0–68.8 vol.% in the temperature range from 300 and 6000 K. The lines represent the CO_2 conversion from thermal equilibrium calculations and the square symbols represent experimentally determined CO_2 conversions for the same H_2 inlet concentrations placed at 2000 K. This temperature is chosen as being close to an upper limit of the RWGS process in order to allow comparison of the CO_2 conversions obtained experimentally to those predicted by the thermal equilibrium calculations.

For the selected temperature of 2000 K the experimental values and those obtained by thermal equilibrium calculation overlap up to $[H_2]$ of 38 vol.%. Above $[H_2]$ of 38 vol.% the CO_2 conversions determined experimentally do not increase for larger $[H_2]$ (a trend already presented in Fig. 5), while the thermal equilibrium calculations predict a further increase of the conversion.

In addition to the CO_2 conversion correlation, a full comparison between the concentrations of CO_2, CO, O_2, H_2, H_2O obtained experimentally (square symbols) with the thermal equilibrium calculation at 2000 K (lines) is presented in Fig. 7. Consistent with Eq. (7), $[H_2O]$ is presented as equal to the experimentally determined [CO]. About 11 vol.% of molecular oxygen are present for pure CO_2 plasma, and with admixed H_2 both the experiment and the calculation show negligible oxygen presence. A very good agreement between the measured and calculated concentrations for the relevant molecules is observed up to $[H_2]$ of 38 vol.%. Above $[H_2]$ = 38 vol.% the discrepancy between the measurements and the thermal calculation consistent with the difference in the CO_2 conversion data shown in Fig. 6(b) is visible. This similarity up to $[H_2]$ of 38 vol.% indicates that the mixture of CO_2 and H_2 in the microwave plasma torch is limited by the upper limit of the thermodynamics of RWGS. This correlation also explains the strong reduction of the CO_2 conversion observed for small H_2 admixtures shown in Fig. 5.

The heat required for the RWGS reaction is provided by the plasma. Up to the $[H_2]$ of 38 vol.% the heat from the plasma is sufficient to drive the RWGS reaction at its upper limit regardless if the H_2 is present in the resonator or added after the plasma. Addition of $[H_2]$ beyond 38 vol.% in the effluent ($[H_2]$ > 38 vol.% in the resonator is not stable) leads to lowering of the temperature of the gas mixture consisting of the hot plasma and the cold (room temperature) H_2 (RWGS reaction zone). A hypothesis is that the lower temperature in the RWGS reaction zone yields results lower than the upper limit of RWGS. Future work to experimentally confirm this hypothesis by measuring the gas temperature in the effluent is envisaged. One way to indirectly test the hypothesis is to increase the average temperature of the plasma (and the RWGS reaction zone) by increasing the microwave power, which is discussed next.

For two conditions, $[H_2]$ of 38 vol.% and 75 vol.%, the microwave power is varied below and above 1.8 kW. The results are shown in Fig. 8(a) as empty squares ($[H_2]$ = 38 vol.%) and as empty triangles ($[H_2]$ = 75 vol.%) on top of data points obtained for 1.8 kW (full circles). Additionally, the CO_2 conversion predicted by the thermal equilibrium calculations at 1000 K (blue line) and 2000 K (green line) is shown. As mentioned previously 2000 K is used as a value close to the upper limit of RWGS and 1000 K is used here as a value close to the lower limit of RWGS.

Increasing the power beyond 1.8 kW at $[H_2]$ = 38 vol.% does not yield larger CO_2 conversions, as the maximum has already been achieved in accordance with RWGS, and additional power is deposited in heat dissipated in the system, as discussed in the next section. In contrast, at 75 vol% $[H_2]$, increasing the power beyond 1.8 kW does result in increased CO_2 conversion. This can be explained by the limit imposed by the thermodynamics of RWGS: at 38 vol.% $[H_2]$, the CO_2 conversion of 50% with 1.8 kW is close to that predicted by thermal equilibrium calculations, while the experimental conversions at 75 vol.% $[H_2]$ are still low when compared to the maximum conversion of 90 vol.%. These observations are more clearly demonstrated in Fig. 8(b). Therefore, the lower CO_2 conversions experimentally obtained above $[H_2]$ = 38 vol.% are due to insufficient power delivered to the plasma, which limits the gas temperatures required to drive additional RWGS reactions between CO_2 and the increasing amount of room temperature H_2 injected after the resonator.

To summarise, comparison of the CO_2 conversion and the outflow gas composition obtained experimentally and determined by thermal equilibrium calculation shows similar values up to $[H_2]$ = 38 vol.% indicating that in this range the admixing of H_2 to the CO_2 microwave plasma can be described well by RWGS thermodynamics. This observations are corroborated by the experiments where the microwave power is increased beyond 1.8 kW at $[H_2]$ = 38 vol.% yielding no change

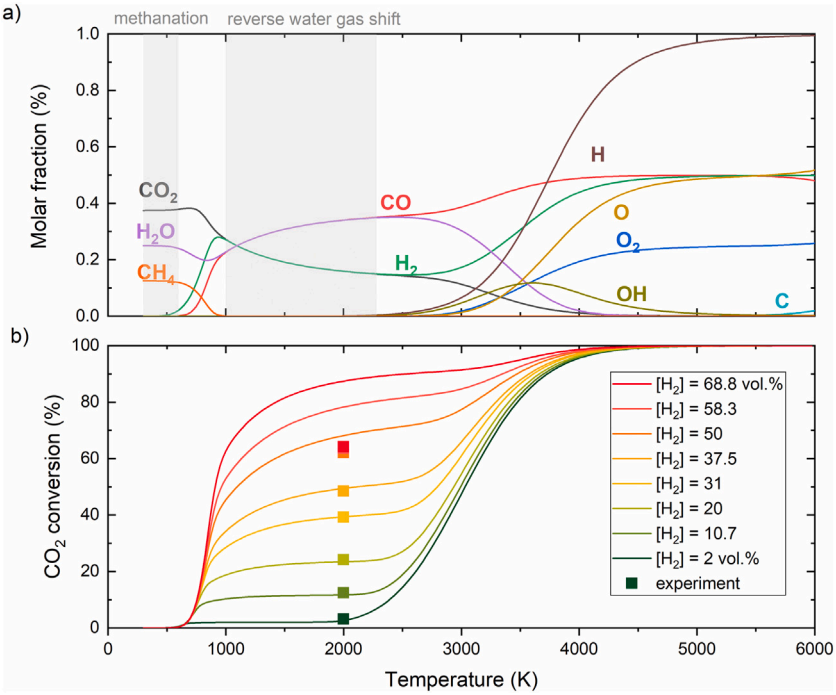

Fig. 6. (a) Molar compositions in the temperature range 300 K to 6000 K obtained with thermal equilibrium calculations for $[H_2]$ of 31 vol.% at 900 mbar, and (b) CO_2 conversion (as defined in Eq. (4)) in the same temperature range for different H_2 inlet concentrations represented by lines. The square symbols represent the experimentally determined conversions for the same H_2 inlet concentrations.

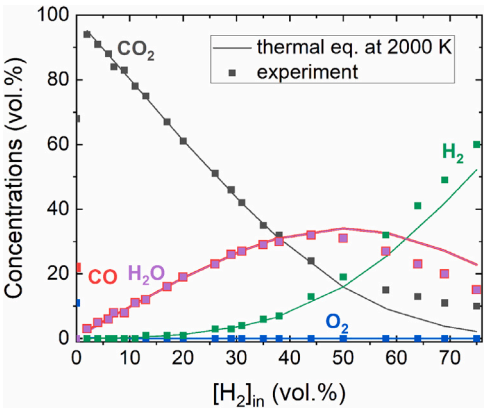

Fig. 7. Concentration of molecules for different H_2 inlet concentrations. Square symbols are for the experimental data, and lines represent values obtained from thermodynamic equilibrium calculations at 2000 K.

in the product gas as the RWGS limit has been reached. In contrast, at 75 vol% $[H_2]$, increasing the power beyond 1.8 kW does result in increased CO_2 conversion towards a higher limit indicated by RWGS. Furthermore, for small H_2 admixtures the trends of the oxygen removal and of the CO_2 conversion limitation observed are consistent with the RWGS process.

3.4. Energy yield

Increasing the microwave power at higher H_2 concentrations to reach the RWGS limit of CO_2 conversion will not necessarily result in a higher energy efficiency. This is demonstrated in Fig. 9 showing the energy yield (relation (13)) on the left ordinate, and the energy efficiency (relation (12)) on the right ordinate. Increasing the power at $[H_2]$ of 38 vol.%, and 75 vol.% results in lower efficiency, since the additional power is only partially channelled to higher conversion and the rest is lost, probably towards heating.

For a fixed power of 1.8 kW the overall trend of the energy yield and efficiency is similar to the trend of the CO_2 conversion shown in Fig. 5. Small amounts of H_2 reduce the efficiency compared to the pure CO_2 case. Increasing the H_2 concentration results in a higher efficiency, surpassing the efficiency of the pure CO_2 plasma at the $[H_2]$ of 20 vol%. For 1.8 kW, the highest efficiency is reached around $[H_2]$ = 65 vol.% resulting in an energy yield of 0.27 $kg_{CO}kWh^{-1}$ and an energy efficiency of 22%. In this concentration range ($[H_2] \approx$ 65–70 vol.%) the H_2/CO ratio in the product gas is in the range of 1.8–2.2 which is suitable for fuel synthesis processes such as the Fischer–Tropsch process [3] as mentioned in the introduction.

For reference, the fuel energy efficiency, which includes the energy stored in both CO and H_2 as defined in Eq. (14), is also calculated. The highest values are obtained for H_2 inlet concentrations in range from 65 vol.% to 75 vol.% yielding values up to $\eta_f = 0.775$. A similar maximum value has been reported in the work by Kuijpers et al. where $\eta_f = 0.7$ is achieved for a CH_4 inlet concentration of 30 vol.% [21].

3.5. Performance comparison

Compared to other methods for O_2 removal, RWGS promoted by H_2 addition to the CO_2 plasma is similar to the carbon bed method, to the extent that both methods remove 99% of O_2 and enhance CO_2 conversion. The product of CO_2 plasma combined with a carbon bed in the effluent is a CO_2 and CO mixture, whereas the RWGS product stream contains CO_2, CO, H_2 and water. The water can be easily removed and reused in combination with a water electrolysis unit. The disadvantage of both methods is requirement for a precursor (H_2 or carbon) that has a strong influence on the overall cost of the produced CO. The reduced oxygen carriers method also requires a precursor since H_2 is typically used in a reduction step. Moreover, this method has not yet been demonstrated for conditions where several slm of oxygen are removed in a closed chemical loop. Regarding the method with MIEC membranes, the main challenge of this method is oxygen

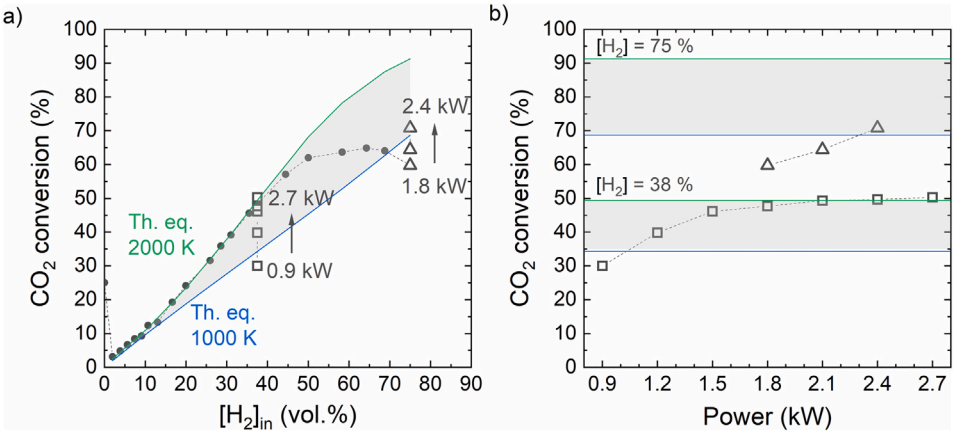

Fig. 8. (a) CO_2 conversion as function of H_2 inlet concentrations for a fixed CO_2 flow rate of 10 slm, and (b) dependency on microwave power. Expansion of Fig. 5 with blue and green lines representing CO_2 conversion from the thermal equilibrium calculation at 1000 K and 2000 K, respectively. The empty symbols obtained at different power levels for H_2 concentration of 38 vol.%, and 75 vol.%.

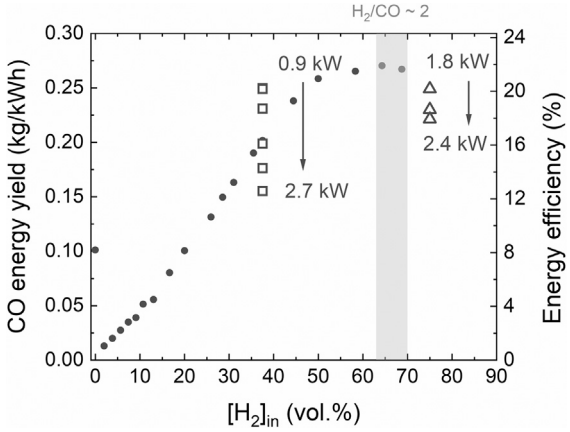

Fig. 9. CO energy yield and energy efficiency for different H_2 inlet concentrations. The full symbols are obtained at a fixed power of 1.8 kW. The empty symbols are for variation of power at H_2 concentrations of 38 vol.%, and 75 vol.%. The shaded area marks conditions for which the $[H_2]/[CO]$ ratio is around 2.

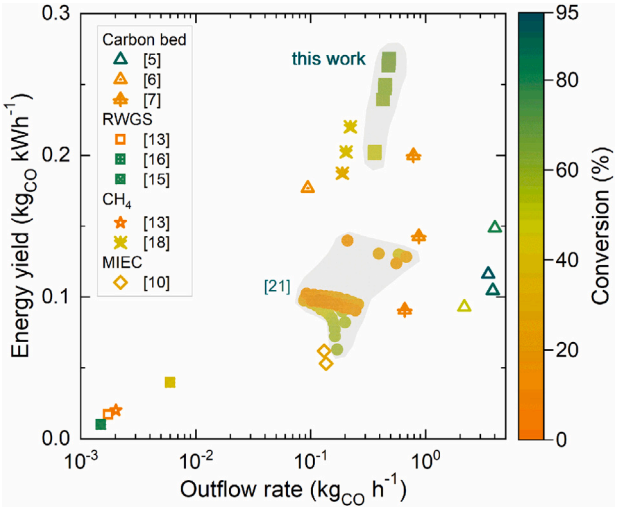

Fig. 10. CO energy yield and CO outflow rate for this work and results from literature on plasma processes only. The colour coding of the data points corresponds to the CO_2 conversion shown on the right. The legend in figure groups the referenced papers based on the method used for O_2 removal: carbon bed, RWGS, methane addition, or use of MIEC membranes.

removal towards 90% and above. The oxygen permeation mechanism is driven by difference of the oxygen partial pressure, thus for low O_2 concentrations, permeation rates are quite low.

To place the results of this work in a perspective with other O_2 removal methods, a compilation of results from the literature is plotted in Fig. 10 along with the results from this work. The efficiency of the process, represented by the energy yield, is plotted against the CO outflow rate (in $kg_{CO}h^{-1}$). If the exact values are not stated in the cited literature, they were calculated using the reported power, the CO_2 flow rate and the CO_2 conversion. The results from literature report on reactors of different sizes, therefore the CO outflow axis is presented using a logarithmic scale. The colour coding of the data points corresponds to the CO_2 conversion with the colour scale shown on the right. The legend in the figure groups the referenced papers based on the method used for O_2 removal: carbon bed, RWGS, methane addition, or use of MIEC membranes. Additionally, results from our previous work without O_2 removal are grouped around Ref. [24].

The comparison demonstrates that the results presented in this work yield the highest energy yields (0.27 $kg_{CO}kWh^{-1}$) so far reported in the literature. It also marks a clear improvement in both the energy yield, and the CO_2 conversion compared to our previous best conversion results [24]. The work of Kuijpers et al. [21] obtained by addition of methane after a microwave CO_2 plasma achieves energy yields of around 0.22 $kg_{CO}kWh^{-1}$, albeit at lower CO outflow rates. The outflow rates of 0.5 $kg_{CO}h^{-1}$ achieved in this work are lower than the results obtained with a gliding arc featuring a carbon bed at 0.9 $kg_{CO}h^{-1}$ [8] and at 4 $kg_{CO}h^{-1}$ [5], albeit at lower energy yield of at 0.2 $kg_{CO}kWh^{-1}$ and 0.15 $kg_{CO}kWh^{-1}$, respectively. These higher outflow rates are directly correlated with higher CO_2 flow rates (110 slm and 25 slm compared to 10 slm used here) and higher applied powers (9.5 kW and 16 kW compared to 2.7 kW used here). Also, consumption of the carbon bed will contribute to the total CO outflow rate, as for each converted CO_2 molecule two CO molecules are generated. This comparison demonstrates that the method of O_2 removal by H_2 admixing to the microwave CO_2 plasma or its effluent is a very efficient process compared to other methods. In the future, experiments it will be conducted to investigate if the efficiency is consistent at higher powers and flow rates.

4. Conclusion

The complete removal of O_2 in addition to CO_2 conversions up to 65% is demonstrated by admixing H_2 in a 2.45 GHz microwave plasma torch. The addition of H_2 gas in CO_2 plasma is achieved either immediately downstream of the resonator or inside the resonator. The results show that the performance is independent of the H_2 inlet position as long as it is close to the plasma where the heat of the plasma is used to drive the Reverse Water Gas Shift (RWGS) process. A large pressure range from 200 to 950 mbar has been tested demonstrating no significant influence of pressure on the performance. Due to its importance for industrial application focus is given on 900 mbar of pressure where a large range of H_2 inlet concentrations (up to 75 vol.%) and powers (up to 2.7 kW) is investigated.

Results show that a concentration as low as 2 vol.% of H_2 in CO_2 is sufficient to reduce O_2 concentration below 0.1 vol.%. This negligible O_2 concentration is measured for the whole range of investigated H_2 admixtures. The CO_2 conversion drops for low H_2 concentrations added to the CO_2 plasma, however above the [H_2] of 20 vol.% the CO_2 conversions exceeded those obtained in pure CO_2 plasma (~25%) reaching highest values of 65%.

The results demonstrate that the mixture of CO_2 and H_2 in the microwave plasma torch is driven by the thermodynamics of RWGS, with the CO and H_2O as a sole products. Both the oxygen removal and limited CO_2 conversion observed for small H_2 admixtures are consistent with the limit of the RWGS process. Furthermore, comparison of the outflow gas composition obtained experimentally and by thermal equilibrium calculation show similar values up to [H_2] = 38 vol.%. As demonstrated with the microwave power variation, the thermal equilibrium for [H_2] admixtures up to 38 vol.% is reached. However for [H_2] above 38 vol.% it has not yet been reached at the investigated power of 1.8 kW, and increase in the power leads to higher CO_2 conversions. This observation corroborates the hypothesis that performance of the plasma torch is defined by the temperature of the plasma and the H_2 gas mixture in the RWGS reaction zone.

The efficiency of the process is assessed using both the energy yield (in $kg_{CO}kWh^{-1}$) and the energy efficiency with respect to the enthalpy of RWGS. Maximum efficiency (at 1.8 kW) is reached at around [H_2] = 65 vol.% resulting in an energy yield of 0.27 $kg_{CO}kWh^{-1}$, and the CO outflow rate of 0.5 $kg_{CO}h^{-1}$. In a similar range ([H_2] ≈ 65–70 vol.%), in addition to [O_2]<0.1 vol.%, the [H_2]/[CO] ratio in the product gas lies in the range between 1.8–2.2 which makes it suitable for synthetic fuel processes such as Fischer–Tropsch.

Plasma conditions with high CO_2 conversions, negligible oxygen concentration in the effluent and a H_2/CO ratio close to 2 suitable for the Fischer–Tropsch process are demonstrated in a microwave plasma torch at atmospheric pressure. The performance comparison demonstrates that the presented method of O_2 removal by H_2 admixing to the microwave CO_2 plasma is a very efficient process compared to other methods yielding the highest energy yields. These results place the plasma torch as a promising process technology to produce gas streams relevant for the synthesis of fuels using downstream processes such as Fischer–Tropsch.

CRediT authorship contribution statement

A. Hecimovic: Writing – original draft, Investigation, Formal analysis, Data curation, Conceptualization. **R. Antunes:** Writing – review & editing, Formal analysis, Data curation, Conceptualization. **C. Kranig:** Writing – review & editing, Formal analysis, Data curation. **A. Meindl:** Writing – review & editing, Conceptualization. **U. Fantz:** Writing – review & editing, Conceptualization.

Declaration of competing interest

The authors declare that they have no known competing financial interests or personal relationships that could have appeared to influence the work reported in this paper.

Acknowledgements

A fruitful discussion with colleagues (M. Bresser, A. Schulz, K. Wiegers, and M. Walker) from IGVP institute at University of Stuttgart is highly appreciated. We are thankful to F. Franco for helping format some of the figures.

Appendix A. Supplementary data

Supplementary material related to this article can be found online at https://doi.org/10.1016/j.jcou.2026.103403.

Data availability

Data will be made available on request.

References

[1] B. de Haart, U. Fantz, A. Hecimovic, A. Schulz, A.N. Munoz, M. Klumpp, Nachrichten Aus der Chem. 69 (6) (2021) 52–59.
[2] R. Snoeckx, A. Bogaerts, Chem. Soc. Rev. 46 (19) (2017) 5805–5863.
[3] H.J. Venvik, J. Yang, Catal. Today (ISSN: 0920-5861) 285 (2017) 135–146, ISSN 0920-5861.
[4] X. Ma, J. Albertsma, D. Gabriels, R. Horst, S. Polat, C. Snoeks, F. Kapteijn, H.B. Eral, D.A. Vermaas, B. Mei, S. de Beer, M.A. van der Veen, Chem. Soc. Rev. 52 (11) (2023) 3741–3777, ISSN 1460-4744.
[5] Z. Li, T. Yang, S. Yuan, Y. Yin, E.J. Devid, Q. Huang, D. Auerbach, A.W. Kleyn, J. Energy Chem. 45 (2020) 128–134, ISSN 2095-4956.
[6] F. Girard-Sahun, O. Biondo, G. Trenchev, G. van Rooij, A. Bogaerts, Chem. Eng. J. 442 (2022) 136268, ISSN 1385-8947.
[7] O. Biondo, K. Wang, H. Zhang, A. Bogaerts, Chem. Eng. J. 507 (2025) 160190, ISSN 1385-8947.
[8] R. Bryssinck, G.J. Smith, C. O'Modhrain, T. Van Assche, G. Trenchev, A. Bogaerts, React. Chem. Eng. 10 (8) (2025) 1910–1923, 2058-9883.
[9] Y. Long, X. Wang, H. Zhang, K. Wang, W.-L. Ong, A. Bogaerts, K. Li, C. Lu, X. Li, J. Yan, X. Tu, H. Zhang, JACS Au 4 (7) (2024) 2462–2473, ISSN 2691-3704.
[10] F. Buck, K. Wiegers, A. Schulz, T. Schiestel, J. Ind. Eng. Chem. 104 (2021) 1–7, ISSN 1226-086X.
[11] R. Antunes, K. Wiegers, A. Hecimovic, C.K. Kiefer, S. Buchberger, A. Meindl, T. Schiestel, A. Schulz, M. Walker, U. Fantz, ACS Sustain. Chem. Eng. 11 (44) (2023) 15984–15993, ISSN 2168-0485.
[12] A. Pandiyan, V. Kyriakou, D. Neagu, S. Welzel, A. Goede, M.C. van de Sanden, M.N. Tsampas, J. CO2 Util. 57 (2022) 101904, ISSN 2212-9820.
[13] R.a. Debek, F. Azzolina-Jury, A. Travert, F. Maugé, Renew. Sustain. Energy Rev. 116 (2019) 109427, ISSN 1364-0321.
[14] R. Aerts, R. Snoeckx, A. Bogaerts, Plasma Process. Polym. 11 (10) (2014) 985–992, ISSN 1612-8850.
[15] L. Liu, S. Das, T. Chen, N. Dewangan, J. Ashok, S. Xi, A. Borgna, Z. Li, S. Kawi, Appl. Catal. B: Environ. 265 (2020) 118573, ISSN 0926-3373.
[16] R. Chaudhary, Plasma enabled chemical value-product pathways from CO2 and H2, chsep=, midc=(Ph.D. thesis), including methanol synthesis, Technische Universiteit Eindhoven, 2019.
[17] J.F. de la Fuente, S.H. Moreno, A.I. Stankiewicz, G.D. Stefanidis, Int. J. Hydrog. Energy 41 (46) (2016) 21067–21077, ISSN 0360-3199.
[18] M. Bresser, S. Wahl, K. Wiegers, A. Schulz, M. Walker, G. Tovar, DPG Tagung, 2024.
[19] K. Jeong, M. Binns, J.-K. Kim, Int. J. Hydrog. Energy 164 (2025) 150859, ISSN 0360-3199.
[20] C.-X. Wang, H.-X. Liu, H. Gu, J.-Y. Li, X.-M. Lai, X.-P. Fu, W.-W. Wang, Q. Fu, F.R. Wang, C. Ma, C.-J. Jia, Nat. Commun. 15 (1) (2024) ISSN 2041-1723.
[21] L. Kuijpers, C.F. van Deursen, Q. Shen, W.A. Bongers, E.J. Devid, M.C. van de Sanden, ACS Sustain. Chemistry; Eng. 13 (32) (2025) 13085–13099, ISSN 2168-0485.
[22] S. Van Alphen, B. Wanten, F. Girard-Sahun, J. Slaets, J. Creel, M. Aghaei, A. Bogaerts, ACS Sustain. Chem. Eng. 12 (42) (2024) 15715–15728, ISSN 2168-0485.
[23] A. Hecimovic, F.A. D'Isa, E. Carbone, U. Fantz, J. CO2 Util. 57 (2022) 101870.
[24] A. Hecimovic, C. Kiefer, A. Meindl, R. Antunes, U. Fantz, J. CO2 Util. 71 (2023) 102473, ISSN 2212-9820.
[25] F.A. D'Isa, E.A.D. Carbone, A. Hecimovic, U. Fantz, Plasma Sources Sci. Technol. 29 (10) (2020) 105009.
[26] E. Carbone, F. D'Isa, A. Hecimovic, U. Fantz, Plasma Sources Sci. Technol. 29 (5) (2020) 055003.

[27] W. Bongers, H. Bouwmeester, B. Wolf, F. Peeters, S. Welzel, D. van den Bekerom, N. den Harder, A. Goede, M. Graswinckel, P.W. Groen, J. Kopecki, M. Leins, G. van Rooij, A. Schulz, M. Walker, R. van de Sanden, Plasma Process. Polym. 14 (2016) 1600126.
[28] A. Hecimovic, F. D'Isa, E. Carbone, A. Drenik, U. Fantz, Rev. Sci. Instrum. 91 (11) (2020) 113501.
[29] E. Mercer, M. Albrechts, R. De Meyer, I. Fedirchyk, E. Morais, S. Bals, A. Bogaerts, Chem. Eng. J. 521 (2025) 166038, ISSN 1385-8947.
[30] B. Wanten, R. Vertongen, R. De Meyer, A. Bogaerts, J. Energy Chem. 86 (2023) 180–196, ISSN 2095-4956.
[31] L. Waldheim, T. Nilsson, IEA Bioenergy Task 33, URL https://task33.ieabioenergy.com/wp-content/uploads/sites/33/2022/06/HeatingValue.pdf.
[32] D.G. Goodwin, H.K. Moffat, I. Schoegl, R.L. Speth, B.W. Weber, Cantera: An Object-oriented Software Toolkit for Chemical Kinetics, Thermodynamics, and Transport Processes, Zenodo, 2024.